THE JOURNAL OF PHYSICAL CHEMISTRY B

Article

pubs.acs.org/JPCB

Organization of T-Shaped Facial Amphiphiles at the Air/Water Interface Studied by Infrared Reflection Absorption Spectroscopy

Christian Schwieger,* Bin Chen, Carsten Tschierske, Jörg Kressler, and Alfred Blume

Institute of Chemistry, Martin-Luther-University Halle-Wittenberg, von-Dankelmann-Platz 4, D-06120 Halle (Saale), Germany

Supporting Information

ABSTRACT: We studied the behavior of monolayers at the air/water interface of T-shaped facial amphiphiles which show liquid-crystalline mesophases in the bulk. The compounds are composed of a rigid *p*-terphenyl core (TP) with two terminal hydrophobic ether linked alkyl chains of equal length and one facial hydrophilic tri(ethylene oxide) chain with a carboxylic acid end group. Due to their amphiphilic nature they form stable Langmuir films at the air/water interface. Depending on the alkyl chain length they show markedly different compression isotherms. We used infrared reflection absorption spectroscopy (IRRAS) to study the changes in molecular organization of the TP films upon compression. We could retrieve information on layer thickness, alkyl chain crystallization, and the orientation of the TP cores within the films. Films of TPs with long (16 carbon atoms: TP 16/3) and short (10 carbon atoms: TP 10/3) alkyl chains were compared. Compression of TP 16/3 leads to crystallization of the terminal alkyl chains, whereas the alkyl chains of TP 10/3 stay fluid over the complete compression range. TP 10/3 shows an extended plateau in the compression isotherm which is due to a layering transition. The mechanism of this layering transition is discussed. Special attention was paid to the question of whether a so-called roll-over collapse occurs during compression. From the beginning to the end of the plateau, the layer thickness is increased from 15 to 38 Å and the orientation of the TP cores changes from parallel to the water surface to isotropic. We conclude that the plateau in the compression isotherm reflects the transition of a TP monolayer to a TP multilayer. The monolayer consists of a sublayer of well-organized TP cores underneath a sublayer of fluid alkyl chains whereas the multilayer consists of a well oriented bottom layer and a disordered top layer. Our findings do not support the model of a roll-over collapse. This study demonstrates how the IRRA band intensity of OH or OD stretching vibrations can be used to retrieve information about layer thickness and refractive indices of the film and how multicomponent IRRA bands can be fitted to retrieve information about the orientation of molecules within the monolayer.

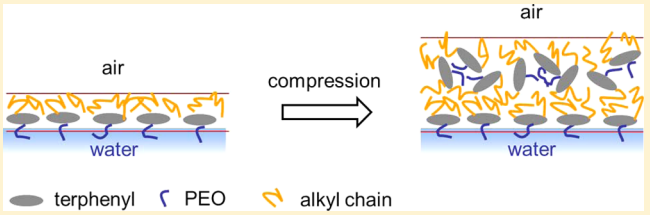

INTRODUCTION

The air/water interface can serve as a template for the self-assembly of amphiphilic molecules. If their hydrophobicity is sufficiently high they form insoluble and compressible Langmuir films. For monolayers at the air/water interface many experimental parameters, such as the surface density of spread molecules, the temperature, or the concentration of subphase additives can be easily controlled and numerous properties of self-assembled films can be collected by different methods. Experimental advantages are the accessibility of the interface and its perfectly flat geometry. Therefore, the behavior of amphiphiles, such as fatty acids or lipids,[1,2] was studied on the air/water interface. In recent years, the interest was growing to study the self-organization of amphiphilic anisometric organic molecules (mesogens) at the air/water interface.[3−16] Well investigated systems are the mesogenic *p*-alkyl substituted cyano-biphenyls[4,5,9,17] and *p*-alkyl substituted cyano-terphenyls.[3,18,19] This research was motivated by the fact that thin organized organic films are of potential use for organic electronics.[20] The studied molecules usually form liquid crystalline mesophases in bulk and show thermotropic mesomorphism.[21] The underlying organization principles also lead to self-organization at the air/water interface and potentially to lyotropic phase transitions upon compression of the formed Langmuir monolayers. An indication for a monolayer phase transition is a plateau region in the surface-pressure/area (π−A) isotherm. An example is the well-known liquid expanded (LE) to liquid condensed (LC) phase transition of fatty acids and phospholipids with sufficiently long acyl chains.[2] The driving force for this transition is the ordering of the acyl chains. π-A isotherms of organic mesogens often show extended plateau regions, occasionally starting after a decrease in π (negative compressibility), i.e. from a metastable state.[22] Such extended plateau regions were also observed without any tendency to increase the molecular order of the monolayer. Diep-Quang and Ueberreiter described the plateau as a "liquid collapse" of the monolayer.[6] The extended plateau regions in the compression isotherms were often interpreted as layering transitions,[4,7,8,22] i.e. the formation of fluid multilayers. Rapp and Gruler[22] showed that this multilayer formation can indeed be understood as a first order phase transition. Layering transitions were also reported for polymer films.[23,24] The

Received: July 4, 2012
Revised: August 29, 2012
Published: August 29, 2012

number of formed layers (n) was usually estimated on basis of the decrease in the molecular area (A_m) within the plateau region ($n = A_m^{beginning}/A_m^{end}$)[7,8,11,22] and was sometimes verified by layer thickness determinations using X-ray reflectivity measurements.[8,11] Different mechanisms were proposed for the multilayer formation, namely a "lifting" and a "roll-over" mechanism. The term "lifting" describes individual molecules being squeezed out from a densely packed monolayer upon further compression and building up layers on top of the initial monolayer. The term "roll-over" was first used by Jeffers et al.[25] It is commonly used to describe a more organized and concerted way to form triple-layers: The densely packed monolayer forms wrinkles upon compression. Within these wrinkles a bilayer is formed that then slides over the monolayer. A scheme of this "roll-over" process was first published by Ries.[15] In recent years it became the preferred model to explain extended plateaus in π-A isotherms in which the A_m was decreased to 1/3 of the initial value.[5,12,13,16,26] Alternatively to multilayer formation, also tilting of the molecules could explain the plateau in the isotherm.[10,13,27]

The aim of this study is to thoroughly investigate phase transitions of two representative mesogenic compounds at the air/water interface. The studied molecules belong to the family of T-shaped facial amphiphiles.[21,28] They consist of a terphenyl core, which is substituted at the middle ring with a hydrophilic side chain. The terminal positions are substituted with hydrophobic alkoxy chains. Monolayer studies of facial T-shaped amphiphiles bearing an oligo(ethylene oxide) side chain ($(EO)_n$) terminated with glycerol[13,16] or Crown ethers[12] and rather short ether-linked alkyl chains (C_{10} and C_{11}) have been reported before. The authors suggested that extended plateaus in the π–A isotherm reflect the formation of well oriented, parallel stacked triple-layers by a "roll-over" mechanism. The amphiphiles presented in this study are facially substituted with an $(EO)_3$ side chain which is terminated by a carboxylic acid group. The two studied molecules differ in the length of the terminal chains which are either decyl (TP 10/3) or hexadecyl (TP 16/3) groups. The chemical structure and a 3D model of TP 10/3 in a dynamic configuration are given in Figure 1. Both substances show thermotropic mesomorphism in the bulk that differs due to the different length of the alkyl substituents (Table 1). At room temperature TP 10/3 can form a monotropic mesophase, whereas TP 16/3 is crystalline. However, both molecules have the propensity to form a smectic mesophase, which is according to Rapp[22] a prerequisite to undergo layering transitions at the air/water interface.

Langmuir isotherms as well as BAM and AFM images of TP 10/3 and TP 16/3 have been reported by Reuter et al.[14] They suggest that TP 16/3 undergoes a crystallization transition within the monolayer, whereas TP 10/3 undergoes a layering transition that results in a well-oriented triple-layer. In this study we perform a more detailed analysis of the transitions and the film structure in the different phases by means of infrared reflection absorption spectroscopy (IRRAS).

IRRAS monitors vibrational frequencies and intensities of molecular moieties at the air/water interface. Vibrational frequencies are sensitive to the organization (conformation, state of binding) of the vibrators.[30−32] It is, for instance, well-known that the frequency of the CH_2 stretching vibrations differ in the LC and the LE phase of lipid monolayers.[33,34] The intensities of vibrational bands are sensitive to the orientation of the vibration dipole with respect to the incoming IR beam. Therefore, it is possible to calculate the orientation of molecules or molecular moieties at the air/water interface by evaluating spectral intensities measured at different angles of incidence (AoI) and polarizations (p or s) of the incoming IR beam.[35,36] Thus, IRRAS can serve as a tool to study organization and orientation of a self-organized film on a submolecular level. As IRRA spectra and Langmuir isotherms are measured simultaneously, it is possible to correlate structural and orientational changes deduced from IRRAS with features of the isotherms, like "spikes" or plateaus. The vibrational bands that we analyzed are indicated in the ATR-IR spectrum shown in Figure 2. From the analysis of the corresponding IRRA bands we deduced information on the alkyl chain organization, the alkyl chain tilt angle, the layer thickness, and the TP core orientation. This information allowed us to conclude on the type of phase transition that leads to the "spikes" in the isotherm of TP 16/3 and to the

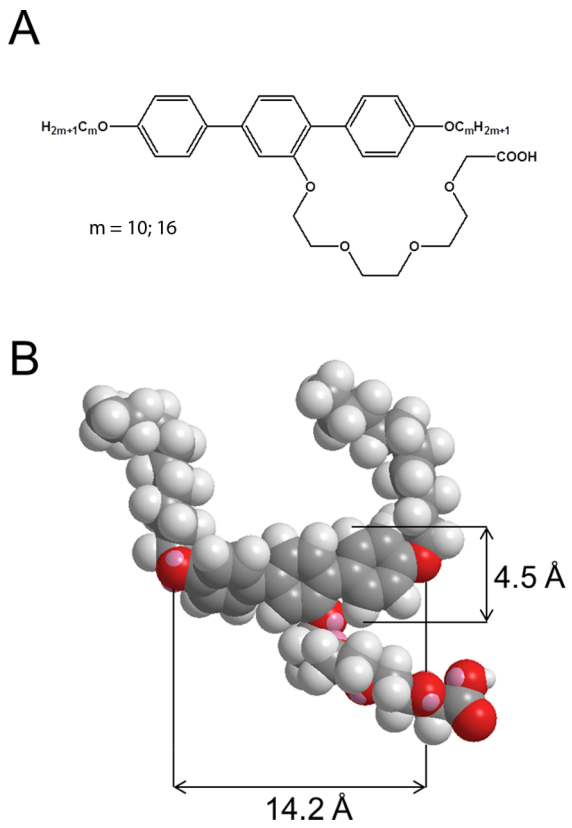

Figure 1. A: Chemical structure of the investigated p-terphenyl derivatives (TP m/3). B: 3D model of TP 10/3 in a dynamic configuration after energy minimization in vacuum.

Table 1. Composition (m = Number of Carbon Atoms in Alkyl Chains; n = Number of Ethylene Oxide Units in the Lateral Chain), Dimension (Length of Alkyl Chains in All-Trans and Length of the Lateral Oligo(ethylene oxide) Chain in Stretched Conformation), and the Thermotropic Phase Sequence of Bulk Material (Col_h: Triangular Cylinder Phase,[29] SmA: Smectic A, Iso: Isotropic, Cr: Crystalline)

abbreviation	m	n	dimensions alkyl/lateral chain [Å]	thermotropic phases/ transition temperatures [°C]
TP 10/3	10	3	11.3/15	Cr 56 (Col_h 46 SmA 56)[a] Iso
TP 16/3	16	3	18.9/15	Cr 79 SmA 100 Iso

[a]Monotropic phases; measured on cooling.

dx.doi.org/10.1021/jp306612k | J. Phys. Chem. B 2012, 116, 12245−12256

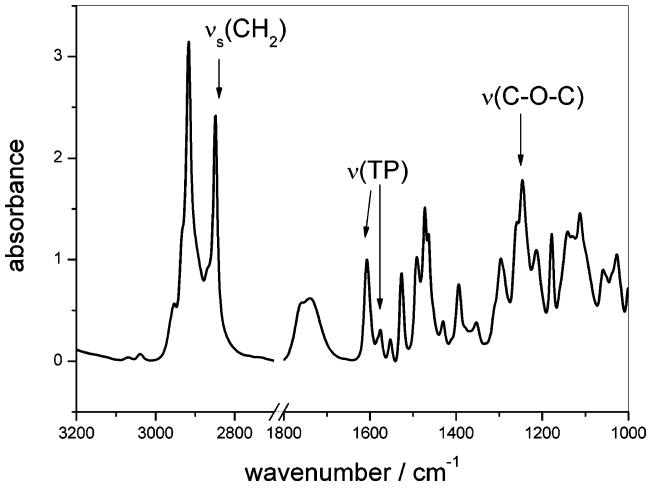

Figure 2. ATR-IR spectrum of dry TP 16/3 at 20 °C. The bands that are analyzed in this study are indicated: $\nu_s(CH_2)$, symmetric CH_2 stretching vibration; ν(TP), combination of C−C stretching vibrations within the terphenyl core; ν(C−O−C), stretching vibration of the ether linkage of the terminal alkoxy chains.

plateau in the isotherm of TP 10/3. We paid special attention to the question whether the extended plateau region can be attributed to a layering transition and by which mechanism, "lifting" or "roll-over", TP 10/3 multilayers are formed. Furthermore the orientation of the TP cores within monolayer and multilayer were analyzed, to check whether the layering transition really leads to the formation of well oriented triple-layers.

MATERIALS AND METHODS

Materials. The T-shaped facial amphiphiles TP 10/3 and TP 16/3 (Figure 1) were synthesized according to the procedure given in Chen et al.[37,38] In our study we use the notation TP m/n, were TP stands for terphenyl, m for the number of carbon atoms in either of the hydrophobic alkyl chains and n for the number of ethylene oxide (EO) units in the facial hydrophilic side chain. Throughout this study n = 3. Lengths of stretched alkyl and EO chains and the thermotropic phase sequence are given in Table 1 and the dimensions of the terphenyl core in Figure 1.

$CHCl_3$ was used in HPLC grade (Carl Roth, Karlsruhe, Germany). Ultrapure water (MiliQ Advantage A10, Merck Millipore, Billerica, MA) or D_2O (Aldrich, 99.9% d) was used for the subphases.

IRRAS Measurements. IRRAS measurements were performed with a Bruker Equinox (isotherms and angle dependent measurements of TP 10/3) and a Bruker Vector 70 FT-IR spectrometer (angle dependent measurements of TP 16/3) equipped with the A511 reflection unit (Bruker Optics, Germany) to guide the IR beam to the air/water interface as well as the reflected beam to an external MCT detector cooled with liquid nitrogen. The angle of incidence (AoI) can be varied between 25 and 70° and the polarization of the IR beam can be set to parallel (p) or perpendicular (s) with respect to the plane of incidence. The size of the IR beam at the point of reflection is 2−5 cm^2, depending on the AoI. Spectrometer and reflection unit were purged with dry air to reduce water vapor absorption bands. In addition, reflection unit and Langmuir trough were placed into a closed plexiglas container in order to maintain a stable atmosphere.

The Langmuir trough system (Riegler and Kirstein, Germany) consisted of a sample (30 × 6 cm^2) and a reference trough (6 × 6 cm^2). Both troughs were thermostatted by a circulating water bath. Measurements were done at 20 °C. Sample trough and reference trough were filled with the same subphase (H_2O or D_2O) of which the level was controlled by a laser being reflected to the surface and kept constant by pumping water from external reservoirs. The sample was dissolved in chloroform and spread dropwise with a microliter syringe onto the water surface in the sample trough. After spreading, evaporation of the chloroform and formation of a homogeneous monolayer was allowed for 10 min. The area available for the monolayer was controlled by two symmetrically movable barriers and is expressed as the molecular area (A_m) in units of [Å^2/molecule]. The surface pressure was detected by a Wilhelmy pressure sensor plate. The trough system is mounted on a shuttle allowing to measure either reference (R_0) or sample (R) reflectivity spectra. The reflectance absorption spectra were then calculated according to RA = $-\log(R/R_0)$.

Two types of IRRAS experiments were performed:

(i) Spectra were accumulated during the continuous compression of the monolayer reducing A_m by 1.55 Å^2/molecule/min. In this case only one reference reflectivity spectrum was taken before the beginning of the compression. After the start of the compression, we continuously recorded sample reflectivity spectra without stopping the compression. 1000 scans were accumulated in 1.5 min and used to calculate one spectrum. Spectra were recorded with a resolution of 4 cm^{-1} and a zero filling factor of 2. The AoI was set to 40° and the polarization to p. The subphase was ultrapure H_2O.

(ii) Angle dependent measurements were performed on TP 16/3 and TP 10/3 at the points indicated in Figure 3A and Figure 6A, respectively. In this case the compression was stopped during the measurements. Spectra were recorded at various angles of incidence, ranging from 26 to 70° in increments of 2°. The film pressure decreased by maximal 2 mN/m during the measurement. A reference reflectivity spectrum was recorded right before each sample spectrum. The subphase level was adjusted before each data acquisition.

Due to the analysis of different reflection−absorption bands and the use of different spectrometers some parameters were specifically adjusted:

Angle dependent measurements on TP 10/3 were performed with D_2O as subphase. Spectra were recorded with p polarization of the IR-beam. 4000 scans were accumulated with a resolution of 8 cm^{-1} and a scanner frequency of 100 kHz. These settings led to a measuring time of 3.5 h for the complete cycle.

Angle dependent measurements on TP 16/3 were performed with H_2O as subphase. Spectra were recorded in p and s polarization. 2000 scans were accumulated in p and 1000 scans in s polarization of the IR-beam with a resolution of 4 cm^{-1} and a scanner frequency of 80 kHz. These settings led to a measuring time of 8.5 h for the complete cycle.

All spectra were calculated with a zero filling factor of 2.

Spectral Simulations and Fits. IRRA spectra were simulated using a MATLAB program. We adopted the optical model of Kuzmin and Michailov[39,40] reported in Flach et al.[41] To simulate spectra with multiple bands, the real (n) and

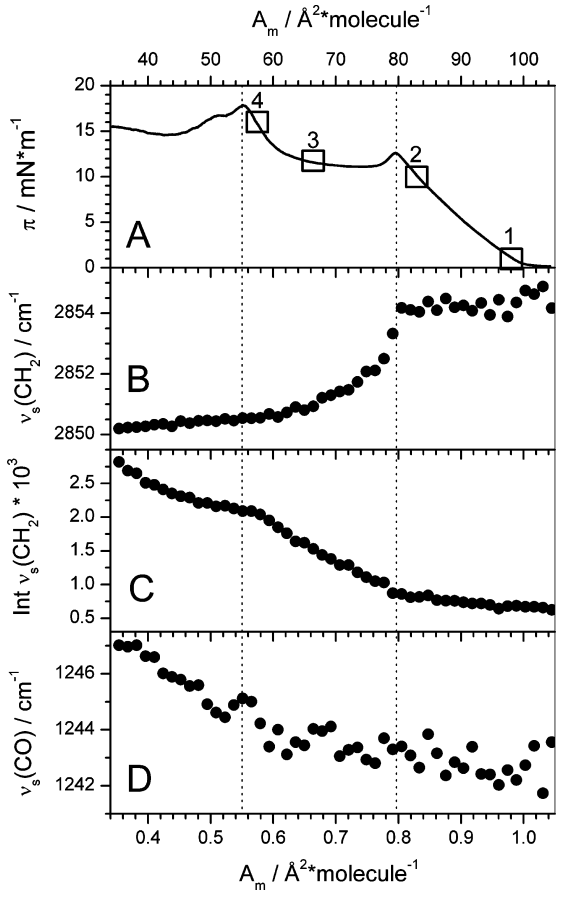

Figure 3. Compression isotherm and IRRAS measurements of TP 16/3 with p-polarized IR light at an angle of incidence of 40°. Spectra were acquired while the film was continuously compressed. A: π–A isotherm, B: position of the symmetric CH_2 stretching vibration, C: intensity of the symmetric CH_2 stretching vibration, D: position of the C–O–C stretching vibration of the terminal ether bond. The squares in A indicate the positions where angle dependent IRRAS measurements were performed.

imaginary (k) parts of the complex refractive indices were calculated according to

$$k^{x,z} = \sum_i k_i^{x,z} \quad (1)$$

$$n^{x,z} = n_{\max} - \sum_i n_i^{x,z} \quad (2)$$

were i denotes the band number and $n_{\max}$ the refractive index of the spread film without contributions of absorption. The indices x and z account for the anisotropy of absorption and denote the components perpendicular and parallel to the surface normal, respectively.

k_i and n_i for a single band are calculated for a Lorentzian shape according to

$$k_i^{x,y} = k_{\max}^{x,y} \cdot \gamma^2/(4\Delta^2 + \gamma^2) \quad (3)$$

$$n_i^{x,z} = -2\Delta \cdot k_{\max}^{x,y} \cdot \gamma/(4\Delta^2 + \gamma^2) \quad (4)$$

where $\gamma = 2\pi c(\text{fwhh})$, $\Delta = 2\pi c(\nu - \nu_0)$, $k_{\max}^{x,z}$ is the absorption coefficient in x or z directions, c is the light velocity, fwhh is the full width at half height, and ν_0 is the frequency of the band center.

The complex refractive index

$$\tilde{n}^{x,z} = n^{x,z} + i \cdot k^{x,z} \quad (5)$$

was then used to calculate the reflectivity of the spread film. The optical constants of the H_2O or D_2O subphase were taken from Bertie et al.[42,43]

Fitting Procedure. Intensity and shape of a reflection absorption band depend on the absorption coefficient k, fwhh, the orientation of the transition dipole moment (TDM) within the molecule α, the molecular tilt angle θ, the polarization and the AoI as well as on d and n. In a typical analysis,[44−49] the band intensity is determined as a function of the AoI. Given that α and n are known, this curve can then be fitted, with θ, k, fwhh, and d being fitting parameters. θ can be determined unambiguously from such a fit, whereas the other three parameters are interdependent. However, this approach is only applicable if the signal-to-noise ratio is high enough and bands do not overlap. As we wanted to determine the molecular orientation from overlapping bands (see the Results and Discussion section), we did not only rely on the band intensities but rather used the complete bands for the fitting. The detailed procedure is described in the Supporting Information.

ATR-IR Measurements. ATR-IR measurements were performed with a Vertex 70 spectrometer equipped with a Bio-ATR II cell and an internal nitrogen-cooled MCT detector (all Bruker Optics, Germany). Spectrometer and cell were purged with dry air during the measurement. The ATR cell was thermostatted by an external water bath. The temperature was controlled by a thermoelement directly in the cell. The sample was pipetted on the ATR crystal as a solution in chloroform. The solvent was allowed to evaporate before the measurement was started. 120 scans were accumulated with a resolution of 4 cm^{-1} to calculate one spectrum after zero filling with a factor 2 and Blackman-Harris appodisation.

DFT Calculations. DFT calculations were carried out with Gaussian 09 (Gaussian Inc., Wallingford, CT). The BP86 functional and 6-31g(d,p)basis set was used. DFT calculations were performed on a reduced molecule, consisting of a terphenyl core, two terminal methoxy groups and one facial hydrophilic group consisting of one EO unit with a charged carboxylate end group (TP 1/1).

RESULTS AND DISCUSSION

TP 16/3. *Measurements at Constant Angle of Incidence and Continuous Compression.* In Figure 3, we present IRRAS measurements on monolayers of TP 16/3. We continuously compressed the TP film starting from an A_m of more than 100 $Å^2$/molecule while accumulating IRRA spectra in p polarization at an AoI of 40°. Only one reference spectrum from the pure water surface was measured at the beginning of the experiment and only 1000 scans were averaged to calculate one spectrum. Although this approach yielded spectra of poor quality (low signal-to-noise ratio, high water vapor contributions) it allowed us to measure one spectrum every 1.8 $Å^2$/molecule, i.e., a total of 30 spectra during the compression.

Figure 3A shows the compression isotherm of TP 16/3. Its shape is very similar to isotherms reported before.[14] It is characterized by two peaks that indicate the formation of different metastable states by overcompression followed by different phase transitions.

To reveal the contribution of the terminal alkyl chains to the phase transition, we evaluated the wavenumber (Figure 3B)

and intensity (Figure 3C) of the symmetric CH_2 stretching vibration ($\nu_s(CH_2)$) as a function of the molecular area (A_m). The frequency of this vibration is an indicator for the alkyl chain organization. It is usually found at about 2850 cm^{-1} for chains in all-trans conformation and shifts to higher wavenumbers as the content in gauche conformers increases.[33,34] At the beginning of the compression isotherm, the $\nu_s(CH_2)$ band was found at 2854−2855 cm^{-1}, which is indicative for fluid alkyl chains, i.e., alkyl chains with high gauche conformer content. The same band position is observed for lipid monolayers in the liquid expanded state or in lipid bilayers in the fluid state.[31,50] The $\nu_s(CH_2)$ frequency stays constant after the first increase of the surface pressure (100 $Å^2$/molecule) and during the first increase in surface pressure until the first peak in the isotherm is reached (80 $Å^2$/molecule). That means in this compression range the alkyl chains stay fluid. Before the lift off they probably lie flat on the water surface between the terphenyl cores. At the lift off, individual molecules come into contact and upon further compression the alkyl chains are squeezed out from the air/water interface and begin to form an alkyl chain sublayer on top of the terphenyl layer at the interface. The position of $\nu_s(CH_2)$ at 2854 cm^{-1} shows that this hydrocarbon sublayer is fluid until the first peak is reached in the π−A isotherm (80 $Å^2$/molecule). In this compression range, i.e., before the first transition peak, the intensity of the $\nu_s(CH_2)$ increases slightly and constantly (Figure 3C). This is due to the increasing surface concentration of alkyl chains as A_m is diminished.

Upon compression beyond the first peak of the π−A isotherm (A_m < 80 Å/molecule), the surface pressure relaxes (Figure 3A) and concomitantly the $\nu_s(CH_2)$ absorption band shifts to lower wavenumbers (Figure 3B). This indicates that the ordering of the alkyl chains begins exactly at the first peak of the compression isotherm, i.e., more trans conformers form, the alkyl chains stretch, and the van der Waals contact between adjacent alkyl chains increases. The decrease in π is a consequence of this more favorable packing of the alkyl chains. In the subsequent pseudoplateau of the isotherm, the ordering of the alkyl chains proceeds. At the end of the pseudoplateau (60 $Å^2$/molecule), the $\nu_s(CH_2)$ absorption band is shifted down to ca. 2850 cm^{-1}, a band position indicative for well-ordered all-trans alkyl chains. As the alkyl chains stretch and order, the intensity of the $\nu_s(CH_2)$ absorption band increases markedly and much more than in the first compression region. The reason is 3-fold: Primarily, the intensity increases because the fwhh of the band decreases due to the more defined conformation of the CH_2 segments, while the integral intensity stays the same. Second, the transition dipole moments of the $\nu_s(CH_2)$ becomes more aligned to the electrical field vector of a p-polarized IR beam which increases their interaction (see below) and third, the overall density increase during the compression leads to an intensity increase proportional to A_m^{-1}. The latter effect alone would increase the band intensity going from 100 to 40 $Å^2$/molecule by a factor of 2.5. The observed increase is, however, much larger with a factor of approximately 4.

This finding corroborates observations made by Reuter et al.[14] via Brewster angle microscopy (BAM). They found spherulithic domains in a TP 10/3 film between the two peaks of the compression isotherm and argued that this was due to a crystallization of the alkyl chains.

Going to lower A_m values, i.e., beyond the end of the pseudoplateau, the $\nu_s(CH_2)$ band does not shift any more, indicating that no more changes occur in the organization of the hydrocarbon sublayer. Also, the second peak in the π−A isotherm does not coincide with a further stretching of the alkyl chains.

The intensity of the $\nu_s(CH_2)$ band slightly increases during the compression in the region of the second peak (60−45 $Å^2$/molecule). The slope is comparable to that at the beginning of the compression, indicating that the increase is only due to an increasing concentration of alkyl chains and no reorganization or reorientation of the alkyl chains take place.

The question remained which kind of film reorganization leads to the second peak in the compression isotherm (55 $Å^2$/molecule). Reuter et al.[14] concluded from BAM images that the second peak is due to film rupture and the formation of three-dimensional structures. Nevertheless, the isotherm is well reproducible including the position of the second peak and a further increase in π that follows the peak upon further compression (not shown). We found that the C−O−C stretching vibrational band (ν(COC)) originating from the vibration of the terminal ether bonds shifts to higher wavenumbers when the film is compressed to A_m values lower than the end of the pseudoplateau, i.e., when the crystallization of the alkyl chains is completed and the second increase in the compression isotherm begins (Figure 3D).

The ν(COC) frequency increase can be due to either a reorganization of the core region (bond angle, coupling to neighboring molecules) or to a change in hydration of the ether bond. To understand the origin of the band shift, we studied the thermotropic phase transitions of bulk TP 16/3 by ATR-IR spectroscopy (Figure 4). From polarization microscopy and X-ray diffraction studies it is known that the liquid crystal undergoes a thermotropic transition from a crystalline phase to a SmA phase at 79 °C.

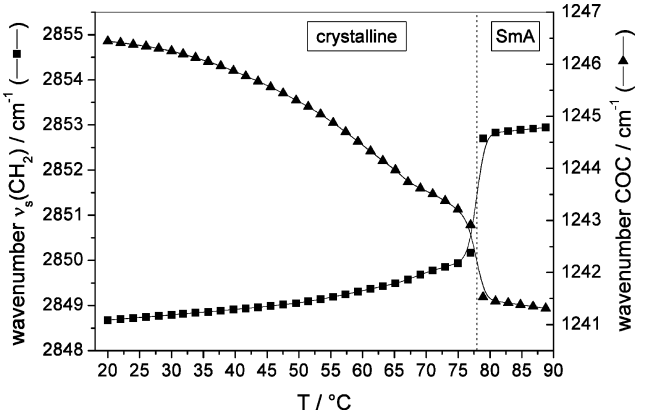

Figure 4. Thermotropic phase behavior of TP16/3 followed by ATR-IR spectroscopy. Maxima of the symmetric CH_2 stretching vibration band (squares) and of the ether bond stretching vibration band (triangles) as a function of temperature.

Figure 4 shows that this transition can be monitored by the shift of the $\nu_s(CH_2)$ and the ν(COC) bands. The maximum of the $\nu_s(CH_2)$ band shifts from approximately 2849 cm^{-1} at 20 °C (cr) to 2853 cm^{-1} at 90 °C (SmA). That corresponds well to the values we detected for the transition of the monolayer (2850 cm^{-1} after the first peak and 2854 cm^{-1} before the first peak). The ν(COC) frequency changes from approximately 1241.5 cm^{-1} at 20 °C (crystalline phase) to 1246.5 cm^{-1} at 90 °C (SmA phase). These values correspond well to the values

dx.doi.org/10.1021/jp306612k | J. Phys. Chem. B 2012, 116, 12245−12256

we determined for completely compressed (A_m = 35 Å^2/molecule) and completely expanded (A_m = 105 Å^2/molecule) TP 16/3 films at the air/water interface, respectively. That means that the shift of this band is not due to a change in hydration but due to a reorganization of the molecules. Furthermore, it can be seen that the temperature dependence is not the same for CH_2 and C−O−C vibrations. Rather, heating of the crystalline phase effects the C−O−C vibrations before the alkyl chains melt. The temperature dependence of ν(COC) even reveals the existence of a pretransition, as can be concluded from the inflection point at approximately 62 °C (Figure 4). That means the melting starts in the core region and then proceeds into the alkyl chain region, or vice versa, upon cooling from the SmA phase, the crystallization starts in the alkyl chain region and then proceeds to the core region. That is exactly what we observe at the air/water interface: Upon compression of the TP 16/3 film first the alkyl chains crystallize (1st peak) and then the core region organizes (2nd peak; see Figure 3B,D).

Angle Dependent Measurements on TP 16/3. We also performed angle dependent IRRAS measurements at selected points of the isotherm, as indicated in Figure 3A. Spectra were recorded with p and s polarization at angles of incidence between 26° and 70° in steps of 2°. A global fit using a theoretical model[40,41] to this set of spectra enabled us to determine (i) the orientation of molecules or molecular moieties[44,45] and (ii) the layer thickness,[30] both being valuable information to develop a structural model. For TP 16/3, it was possible to fit angle dependent spectra in the range of the symmetric and antisymmetric CH_2 stretching vibrations to retrieve the tilt angle of the alkyl chains after they adopted a stretched all-trans conformation (positions 3 and 4 in Figure 3A; experimental and simulated spectra are available in the Supporting Information).

Orientational angles determined at position 1 and 2 cannot be interpreted as fixed tilt angles of the alkyl chains, because the alkyl chains are still fluid. Rather, the angle reflects the average orientation of the CH_2 groups, i.e., the angle between the interface normal and the normal of the plane defined by the 3 atoms of a CH_2 group.

At points 1−4 in Figure 4A the layer thickness was determined from a fit of the OH-stretching vibration (3000−3800 cm^{-1}) originating from the H_2O subphase. For the layer thickness determination the refractive index of the film was set to 1.53, which is the value we determined for a TP 10/3 monolayer (see below). For all calculations we assumed the film to be optically isotropic and used only one effective refractive index (for discussion see the SI). The parameters we determined from the fit of the angle dependent measurements are summarized in Table 2.

The determined layer thickness is increasing constantly from 12 Å at an A_m of 98 Å^2/molecule to 19 Å at 57 Å^2/molecule. This is close to the values that can be calculated from the molecular volume of the alkyl chains and the terphenyl unit, according to

$$d = v_{molecule}/A_m = (v_{alkane} + v_{TP})/A_m \text{ Å} \quad (6)$$

The molecular volume of a primary alkyl chain can be approximated by the following equation:[51]

$$v_{alkane} = (27.4 + 26.9n) \text{ Å}^3 \quad (7)$$

Table 2. Layer Thickness (d_{IRRAS}) and Tilt Angle of Alkyl Chains ($\theta_{IRRAS}(CH_2)$) Calculated from Angle Dependent IRRAS Measurements of TP 16/3 and a Predicted Layer Thickness, Calculated by eq 6-8 (d_{calc}) at Positions Indicated in Figure 3[a]

position	A_m/Å^2 molecule^{-1}	$\theta_{IRRAS}(CH_2)$/°	d_{IRRAS}/Å	d_{calc}/Å
1	98	70*	11.8	12.5
2	83	67*	13.9	14.7
3	66	49	16.2	18.6
4	57	51	19.4	21.5

[a] n was set to 1.53 for the fit of angle dependent IRRA spectra. This value was determined from the fit of the OD stretching vibrations of a TP10/3 monolayer (see below). *Values cannot be interpreted as alkyl chain tilt but as average orientation of the CH_2 segments, defined as orthogonal to the transition dipole moments of $\nu_s(CH_2)$ and $\nu_{as}(CH_2)$.

with n being the number of carbon atoms. This gives a volume of 458 Å^3 per hexadecyl chain (n = 16). If we assume the volume of a terphenyl unit to be given by

$$v_{TP} = 10^{24}M/(\rho N_A) \approx 310 \text{ Å}^3 \quad (8)$$

with M being the molar mass, ρ the density, and N_A the Avogadro number, the volume of the whole molecule can be approximated to 1216 Å^3. The volume of the hydrophilic side chain has been disregarded in these calculations, because due to its refractive index being too close to that of the aqueous subphase it cannot be detected by IRRAS. The layer thickness calculated with these assumptions is given in in the last column (d_{calc}) of Table 2. The values are somewhat higher than the values determined from IRRAS, which can have different reasons: (i) the assumed average refractive index used for the IRRAS fitting procedure is too high, (ii) the estimated molecular volumes are too high, and (iii) possible volume compressibility and refractive index changes upon compression were neglected. However, from the determined layer thicknesses it is reasonable to assume that throughout the compression range from 98 Å^3/molecule to at least 57 Å^3/molecule an alkyl chain layer is formed on top of a terphenyl layer.

It is furthermore interesting to determine, how the alkyl chains are organized within this layer after their crystallization. Therefore, the alkyl chain tilt angle was determined from the CH_2 stretching vibrational bands recorded at different AoI. A tilt angle of 49° with respect to the layer normal was determined at a A_m of 66 Å^3/molecule, i.e., after crystallization of the alkyl chains (position 3 in Figure 3A and Table 2). If we assume the hexadecyl chain to be 21 Å in length and 21 Å^2 in cross sectional area[51] this tilt angle results in a thickness of the hydrocarbon layer of 13.7 Å and an area demand of 32 Å^2 per alkyl chain. The subtraction of the thickness of the alkyl layer from the total film thickness gives a thickness of the terphenyl layer of 2.4 or 4.9 Å (using d_{IRRAS} or d_{calc}, respectively). This corresponds to the height of a terphenyl core lying flat at the air/water interface. The two alkyl chains of one TP 16/3 molecule would cover an area of 64 Å^2, which is close to the A_m of 66 Å^2/molecule at which the tilt angle was determined. This shows that the alkyl layer consists of tilted, densely packed alkyl chains in all-trans conformation. A model of the organization of the TP 16/3 monolayer at position 3 that summarizes all the discussed information is shown in Figure 5.

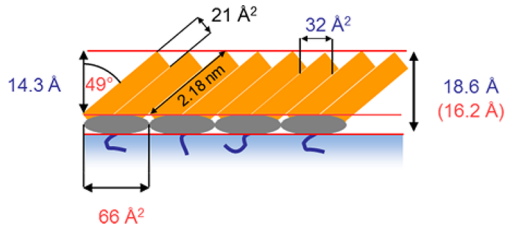

Figure 5. Model of the organization of TP 16/3 at the air/water interface at A_m = 66 Å^2/molecule. Parameters written in red are determined by IRRAS and film balance measurements. Parameters written in black are geometrical parameters according to Isralelachvili.[51] Parameters written in blue are calculated as combination of the other two sets of parameters as described in the text.

Upon further compression (position 4) the tilt angle of the alkyl chains does not seem to change significantly (49° vs 51°) whereas the layer thickness slightly increases. This might be due to an increase in TP layer thickness by tilting of the TP cores or due to molecules being squeezed out from the densely packed monolayer.

TP 10/3. *Measurements at Constant Angle of Incidence and Continuous Compression.* Also with the TP derivative with shorter alkyl chains, TP 10/3, we performed IRRAS measurements at constant angle of incidence while the film was compressed continuously. The compression isotherm is presented in Figure 6A. Although the only difference to TP 16/3 is the length of alkyl chains, the Langmuir isotherm is remarkably different. After an initial increase, it shows a long plateau at a pressure π = 22 mN/m, an indication for a first order phase transition. The TP 10/3 isotherm shows no overcompression peaks as present in the isotherm of TP 16/3. To check whether the alkyl chains form an ordered LC-like phase in the plateau region, we evaluated the position of the $\nu_s(CH_2)$ stretching vibration as described above. The result is shown in Figure 6B. From the beginning (90 Å^2/molecule) until the end (25 Å^2/molecule) of the compression the $\nu_s(CH_2)$ wavenumber decreases only from 2856 to 2854.5 cm^{-1}, indicating that the alkyl chains stay fluid in the complete compression range. Thus, alkyl chain ordering is not the reason for the appearance of the plateau region. Apparently, the decyl chains of TP 10/3 are too short to crystallize under the chosen conditions.

This is consistent with the thermotropic behavior of the TP derivatives in bulk. While TP 16/3 is crystalline at RT and melts only at 79 °C into a SmA phase (seeFigure 4), TP 10/3 forms liquid crystalline monotropic mesophases at RT (Col_h). A SmA phase can form between 46 and 56 °C and at higher temperature TP 10/3 is isotropic (see Table 1). We also performed IR-ATR measurements of bulk TP 10/3 to check for changes in band positions. This is shown in Figure 7. In all phases, the alkyl chains are fluid, as can be concluded from the frequency of the $\nu_s(CH_2)$ band. The finding of fluid alkyl chains in the complete compression range of TP 10/3 film supports the report of Reuter et al.,[14] who stated that alkyl chains of TP 10/3 films do no crystallize under compression. They found fluid domains in BAM images taken in the plateau region of the compression isotherm as well as in AFM images of films transferred to solid substrate at the same compression state. Also the wavenumber of the ν(COC) band shifts only slightly with temperature indicating no major reorganization in the region of the ether groups.

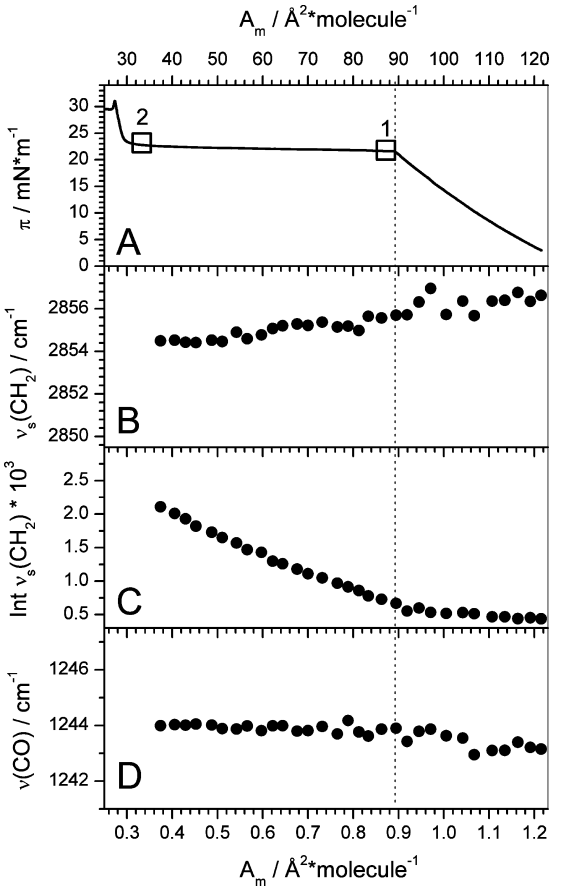

Figure 6. Compression isotherm and IRRAS measurement of TP10/3 with p-polarized IR light at an angle of incidence of 40°. Spectra were acquired while the film was continuously compressed. A: π–A isotherm, B: position of the symmetric CH_2 stretching vibration, C: intensity of the symmetric CH_2 stretching vibration, D: position of the C–O–C stretching vibration of the terminal ether bond. The squares in A indicate the positions where angle dependent IRRAS measurements were performed.

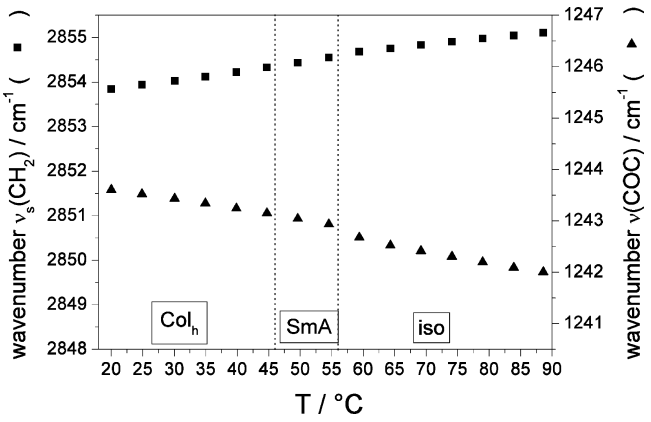

Figure 7. Thermotropic phase behavior of TP 10/3 followed by ATR-IR spectroscopy. Maxima of the symmetric CH_2 stretching vibration band (squares) and of the ether bond stretching vibration band (triangles) as a function of temperature. Scales are chosen the same as in Figure 4 for the sake of comparison.

The $\nu_s(CH_2)$ intensity (Figure 6C) increases slightly upon compression between the lift off and the beginning of the plateau. This increase is expected and can be attributed to the

dx.doi.org/10.1021/jp306612k | J. Phys. Chem. B 2012, 116, 12245–12256

increase in concentration, as the area is diminished. At the beginning of the plateau the slope increases slightly. While A_m is decreased 2.4-fold within the plateau region, the $\nu_s(CH_2)$ intensity increases 3.1-fold. As the alkyl chains stay fluid over the complete compression range neither a change in conformation (gauche → trans) nor a change in orientation should lead to higher band intensities. Therefore, we suggest that a change in reflectivity, due to a change in the optical properties of the film is influencing the $\nu_s(CH_2)$ intensity. The refractive index might change due to a reorientation of the terphenyl cores, which are optically anisotropic, i.e., their refractive index is higher in direction of the molecular director than perpendicular to it.[52,53] Also, dehydration of the hydrophilic side chains might lead to a change in the refractive index. Dehydration might occur when the side chains are pulled out from the aqueous subphase due to multilayer formation. The intensity of the OH stretching band changes in the same manner as the intensity of the $\nu(CH_2)$ bands do. Thus the same interpretation has to apply for the intensity changes of both bands. The only parameters that influence the intensity of the OH-stretching vibrational band are the refractive index n and layer thickness d. This supports the hypothesis that a change in the refractive index is the reason for the stronger increase in band intensities with the beginning of the plateau in the compression isotherm.

Furthermore, we checked whether we see any changes in the organization of the ether bonds that could be an indication for terphenyl core reorganization. Figure 6D shows that the position of the ν(COC) band is constant in the complete compression range. We conclude that no crystallization neither of the alkyl chains nor in the core region occurs during the compression of TP 10/3 films.

Angle Dependent Measurements on TP 10/3. The question remains what kind of transition leads to the long plateau in the compression isotherm of TP 10/3. The A_m value at the beginning of the plateau (89 Å^2/molecule) is a factor of 3 larger than the A_m value at the end of the plateau (29.7 Å^2/molecule). Isotherms of similar shape and A_m relations have been reported for other systems.[5,6,13,16] The A_m reduction to 1/3 of the original value often leads to the conclusion that a fluid triple-layer is formed by a "roll-over" mechanism. This model assumes that the densely packed monolayer bends up under compression and forms a bilayer that then slides over the existing monolayer.[5,13,15,16,25] To check whether this assumption is true for TP 10/3 films we performed angle dependent IRRAS measurements at beginning and end of the plateau. These measurements allow us to determine (i) the layer thickness and the refractive index of the film and (ii) the orientation of the rigid TP cores with respect to the water surface. The results are summarized in Table 3. The tilt of the alkyl chains was not determined because they are fluid, i.e., unorganized over the complete compression range.

Table 3. Fitting Parameters of the Fit of Angle Dependent IRRA Bands at the Beginning and the End of the Plateau of the Compression Isotherm of TP 10/3

parameter	beginning (A_m = 78 Å^2/molecule)	end (A_m = 33 Å^2/molecule)
film thickness (d in Å)	15	38
refractive index (n)	1.53	1.54
tilt of TP (θ_{TP} in °)	88	69

Layer Thickness. The angle dependent measurements of TP 10/3 were performed on D_2O as subphase, because the spectral range which is usually shielded by the OH bending vibration of the aqueous subphase[31] overlaps with the range of the TP ring vibrations (see below). Thus we used the OD stretching vibration in the range of 2300 to 2800 cm^{-1} to determine the layer thickness at the beginning (87 Å^2/molecule) and the end (33 Å^2/molecule) of the plateau of the compression isotherm. At the beginning of the plateau, we calculate a layer thickness of 15 Å. This value agrees well with the model of a densely packed monolayer of TP cores lying flat on the water surface (thickness ca. 4.5 Å) underneath a fluid hydrocarbon layer of decyl chains. A decyl chain in stretched all-trans conformation has a volume of 298.[51] The volume of a fluid decyl chains should be similar, even though they have gauche conformations in the chain which reduces their effective length. At the beginning of the plateau, the available area per fluid alkyl chain is ca. 43.5 Å^2. This would give an effective alkyl chain length, i.e. a thickness of the hydrocarbon layer of ca. 6.8 Å. Probably, the hydrophilic oligo(ethylene oxide) chains that anchor the molecules to the sub phase will contribute to the determined layer thickness and account for the remaining 3.7 Å.

At the end of the plateau (33 Å^2/molecule), we determined a layer thickness of 38 Å. This is equivalent to a 2.5-fold increase in layer thickness. It is far more than a monolayer model could explain, even if the TP cores would tilt and alkyl chains would be more stretched. The only conformation and orientation that would give such a monolayer thickness is a molecule with completely stretched chains oriented perpendicular to the water surface. This is highly unlikely because one alkyl chain would face the water surface, whereas the hydrophilic chains would be lift off from the water surface and the conformation of the decyl chain would be all-trans in contradiction to the observed fluid behavior of the chain. Therefore, the only reasonable model is the formation of a TP 10/3 multilayer during the compression within the plateau region. The same conclusion was drawn by Reuter et al.[14] on the basis of AFM and XRR measurements. The 2.5-fold increase in layer thickness correlates well with the 2.6-fold area decrease between the 2 points of measurements. This means that the layer thickness increases proportional to the A_m decrease. Therefore, one can assume that the layer thickness increase at the end of the plateau is 3-fold. The conclusion that a triple layer of three parallel stacked monolayers is formed is tempting. To check whether this is the case we determined the tilt of the TP cores by angle dependent IRRAS measurements.

Orientation of TP Cores. The terphenyl moiety has several in-plane stretching vibration modes in the spectral region of 1300−1600 cm^{-1}. The most prominent ones located at 1490, 1527, and 1607 cm^{-1} can be well distinguished in the ATR-IR spectra shown in Figure 8A. On a D_2O subphase the TP ring vibrational bands are visible in the IRRA spectra recorded in p polarization and at different AoI at the beginning (Figure 8B) and the end (Figure 8C) of the plateau (spectra recorded at position 1 and 2 in Figure 6A, respectively). However, the bands are less intense and less resolved than in the ATR-IR spectra. The carbonyl stretching vibrational band, located at 1730 cm^{-1} is missing in the IRRA spectra. This shows that the carboxylic acid end group of the hydrophilic side chain deprotonates at the water surface. The resulting carboxylate gives rise to an antisymmetric $\nu_{as}(COO^-)$ and a symmetric $\nu_s(COO^-)$ stretching vibration, located at ca. 1590 and 1400 cm^{-1}, respectively. The antisymmetric band should overlap

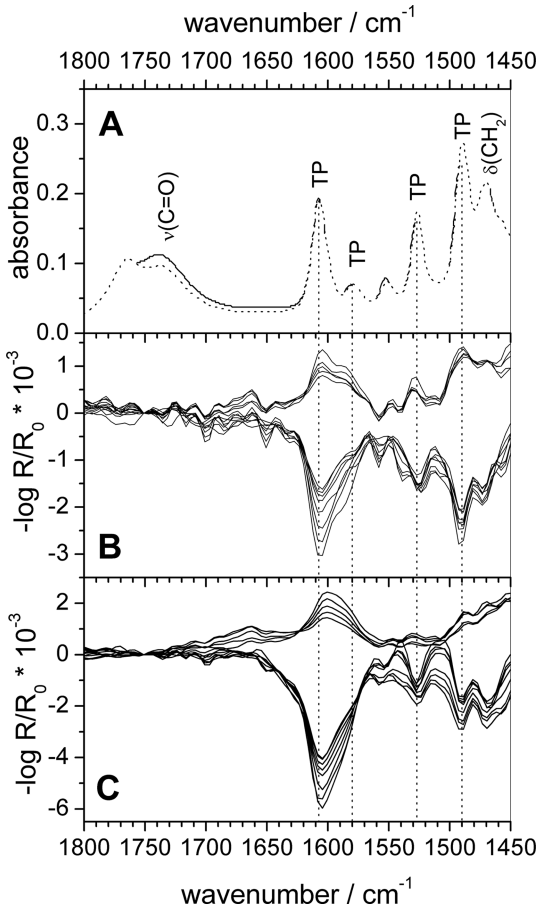

Figure 8. A: ATR-IR spectra of bulk TP 10/3 at 20 °C (bold) and 88 °C (dotted). B: Angle dependent IRRA spectra of TP 10/3 films at the air/water interface at the beginning of the plateau. C: Same as in panel B but at the end of the plateau.

with the most intense TP ring vibrations (1607 and 1580 cm^{-1}). Equally, the TP vibration at 1490 cm^{-1} overlaps with the CH_2 deformation vibration (1467 cm^{-1}). Nonetheless, the direct comparison of panels B and C in Figure 8 shows that the dependence of the TP band intensities on the AoI is different at the beginning and the end of the plateau. While at the beginning of the plateau the band intensities change from negative to positive at the Brewster angle, at the end of the plateau positive intensities of bands recorded above the Brewster angle are low. This is especially well seen for the band at 1527 cm^{-1}, which is free from overlaps. This different angle dependency shows that there must be a reorientation of the TP cores during the compression within the plateau region.

To retrieve more quantitative information on the tilt of the TP cores, we fitted simulated spectra to the experimental ones in the range of the most prominent band between 1570 and 1640 cm^{-1}. This band is a superposition of 3 components: two TP ring vibrations (TP1 and TP2) and the antisymmetric COO^- stretching vibration $\nu_{as}(COO^-)$. In order to generate meaningful fits, as much parameters as possible have to be fixed. Therefore, the positions of the TP bands as well as the ratio of their absorption coefficients were set to the values determined from the ATR-IR spectra. The angles of the TDMs with respect to the molecular director were determined by DFT calculations. The position of the $\nu_s(COO)$ band was allowed to vary in a small spectral window and for the COO^- tilt angle we assumed an isotropic distribution. Furthermore, d and n were used as determined from the OD band fits (see Table 3). Thus, only the TP tilt angle θ_{TP}, the absorption coefficients k_{TP1} and k_{COO} and the fwhh's remain free fitting parameters. With this set of parameters we performed a global fit including all spectra measured at different AoI at the beginning of the plateau (position 1 in Figure 6A). The result is shown in Figure 9A.

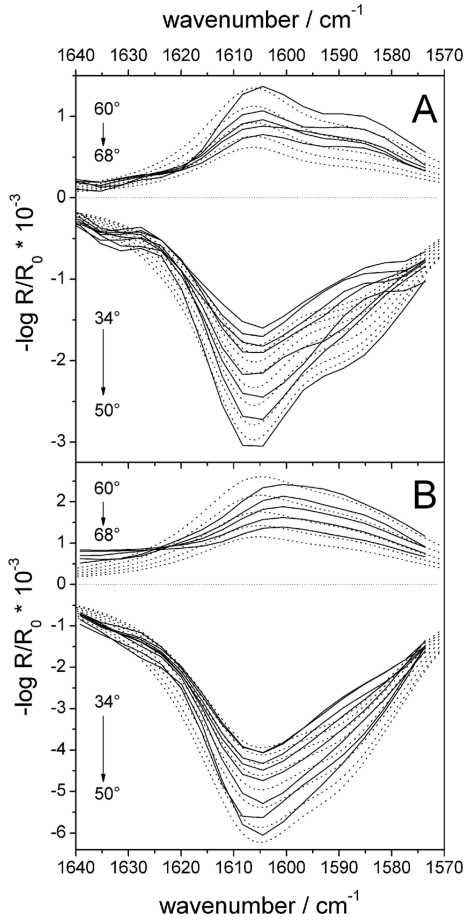

Figure 9. Experimental (bold lines) and simulated (dotted lines) angle dependent IRRA spectra of a vibration of the terphenyl core of TP 10/3 at A: the beginning of the plateau and B: the end of the plateau of the compression isotherm. Angles of incidence were varied between 34° and 68°. Spectra were taken with p-polarized IR-light. Tilt angles in the simulations are A: 88° and B: 69°.

This fit gives a TP tilt angle of 88° with respect to the layer normal, meaning that the TP cores lie flat on the water surface. This is consistent with the determined layer thickness (see above) and the model published by Reuter et al.[14]

The same fitting procedure was applied for spectra recorded at the end of the compression isotherm (position 2 in Figure 6A). We assumed that the absorption coefficients k_{TP1}, k_{TP2}, and k_{COO} did not change during the compression and set them to the values determined at the beginning of the plateau. This reduces the free parameter to only θ_{TP}, and the fwhh's. The result is shown in Figure 9B. The determined average tilt angle of the TP cores at the end of the plateau is 69°. That means that the TP cores indeed change their orientation upon compression in the plateau region of the isotherm. They lose the perfectly flat alignment during the transition from a monolayer to a multilayer. To prove that other orientations of the TP cores do not fit the data equally well, we performed

dx.doi.org/10.1021/jp306612k | J. Phys. Chem. B 2012, 116, 12245−12256

simulations with the same parameters as at the beginning of the plateau (θ_{TP} = 88°) and as well with a perpendicular orientation of the molecules (θ_{TP} = 0°). To compare the different simulations the integral band intensities of experimental and simulated bands were plotted as a function of the AoI (Figure 10B). It can be seen that simulations with parallel or perpendicular molecules fit the data much worse than the best fit with θ_{TP} = 69°. Consequently, the model of a "roll-over" mechanism, which would lead to a triple-layer with all TP cores being parallel to the air/water interface, cannot be confirmed.

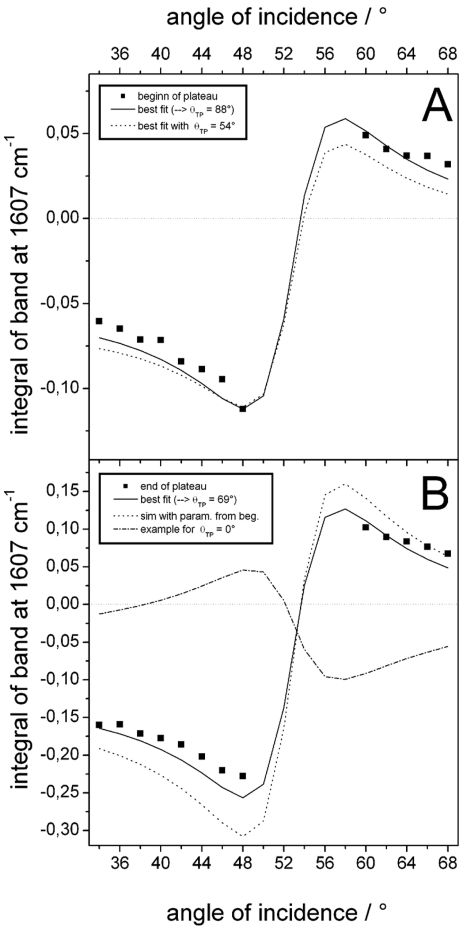

Figure 10. Integral intensities of experimental (squares) and simulated (lines) vibration bands of TP 10/3 (1570 to 1640 cm^{-1}, see Figure 9) at A: the beginning of the plateau and B: the end of the plateau in the compression isotherm. Solid lines show the best fits that yield a tilt angle of 88° in A and 69° in B. Simulations with other tilt angles are additionally shown: dotted line in A: 54°, dotted line in B: 88°, point-dotted in B: 0°.

Equally, it can be excluded that the molecules tilt up to give a monolayer of molecules perpendicular to the water surface.

An average tilt angle of 69° could be explained by a double layer with tilted TP units and fluid alkyl and ethylene oxide chains, which would fit into the 38 Å layer thickness that was determined. But this model is not reasonable, because the hydrophilic part of the upper monolayer would face the air. Therefore, the following model appears to be more reasonable: the lower monolayer maintains its orientation of TP cores parallel to the water surface, still being anchored to the water subphase by the ethylene oxide side chains. Molecules that are squeezed out from this monolayer by compression lose their orientation. They build a second unordered layer on top of the first monolayer. This second layer consists of isotropically distributed TP cores and fluid ethylene oxide chains at the inside and fluid alkyl chains, facing air and the lower monolayer at the outside. At the end of the plateau, this unordered top layer has exactly the thickness of two monolayers and cannot grow further because then segregation in an alkyl chain layer and a TP/EO layer would not be possible anymore. The model of a disordered layer with defined thickness is in line with the report of Chen et al. about lamellar isotropic mesophases (Lam_{iso}) of similar liquid crystals, having a bola-like architecture.[54] Furthermore, the determined average tilt angle of 69° can also be well explained by such a model. At the end of the plateau the lower layer consists of one-third of the molecules having an average tilt angle of 90°. The upper unordered layer consists of 2/3 of the molecules, which contribute to the average tilt with 54°. The average tilt is then given by θ_{TP} = (90° + 2*54°)/3 = 66°. As the angle dependent measurements were not performed exactly at the end of the plateau, the contribution of the lower oriented monolayer could be higher. As we determined a 2.5-fold increase in layer thickness, the average tilt would be given by θ_{TP} = (90° + 1.5*54°)/2.5 = 68°. This is very close to the value we determined by band fitting and supports our model for the orientation of the molecules. A scheme of the proposed organization of TP 10/3 at the air/water interface at the beginning and the end of the plateau is presented in Figure 11.

CONCLUSIONS

We examined the compression isotherms at the air/water interface of two homologous T-shaped facial amphiphiles with terphenyl cores.[12,13,16] Organization and orientation of the molecules within the film was studied by IRRAS. We demonstrated that IRRAS is a versatile and powerful means to study molecular orientation of molecules at the air/water interface. Due to the different length of terminal alkyl chains the two analogues show remarkably different transitions upon compression. The derivative with long alkyl chains (TP 16/3) undergoes a phase transition within the monolayer whereas the

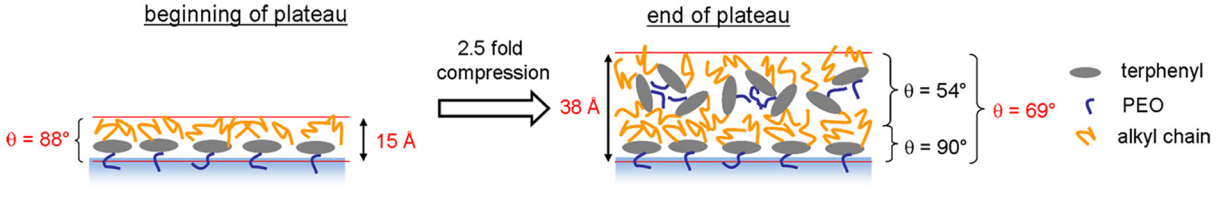

Figure 11. Molecular organization of TP 10/3 in a monolayer at the beginning of the plateau of the compression isotherm (left) and a multilayer at the end of the plateau of the compression isotherm (right). The given tilt angles θ are the tilt angles of the TP cores with respect to the layer normal. Values printed in red are determined by IRRAS measurements.

dx.doi.org/10.1021/jp306612k | J. Phys. Chem. B 2012, 116, 12245−12256

derivative with short alkyl chains (TP 10/3) undergoes a layering transition.

TP 16/3 forms a fluid phase at A_m > 80 Å^2/molecule and an ordered phase at lower molecular area. This was unambiguously deduced from the position of the $\nu_s(CH_2)$ IRRA band. The alkyl chains in these phases behave as in the LE and LC phases formed by fatty acids or lipids.[33,34] This finding supports the hypothesis of Reuter et al.,[14] who observed in BAM images spherulitic domains in the condensed phase of TP 16/3. By means of angle dependent IRRAS, we could furthermore determine the layer thickness at various positions of the compression isotherm as well as the tilt angle of the alkyl chains in the condensed state. On basis of these values, we propose a model of the organization of the condensed monolayer at a molecular level (Figure 5). An interesting feature of the π-A isotherm is a characteristic "spike" at the point of the phase transition (80 Å^2/molecule). This shows that the system enters a metastable state before the condensed phase is formed,[22] i.e., there is an activation barrier for the formation of the condensed phase.[6,22] This activation barrier might be due to a (re)-organization of the TP cores, that might be necessary for allowing the alkyl chains to crystallize. A second "spike" in the π-A isotherm of TP 16/3 at 55 Å^2/molecule could be attributed to a second crystallization step in the core region by monitoring the shift of the C−O−C stretching vibration of the terminal ether linkage. Films of TP 10/3 stay fluid over the complete compression range. No crystallization could be detected by IRRAS, neither for the alkyl chains, nor the core region. No metastable phases were detected during compression. Rather, the isotherm shows an extended plateau region, reflecting a layering transition.

We determined the type of layering transition in the plateau region of the TP10/3 isotherm using IRRAS. By angle dependent measurements, we could determine layer thickness and the average tilt angle of the TP cores at the beginning and the end of the plateau. The ratio of the areas at the beginning and the end of the plateau suggest that a triple-layer is formed. The same conclusion was drawn from the calculated values for the layer thicknesses, which are 15 Å at the beginning and 38 Å at a 2.5-fold reduced area (nearly the end of the plateau). At the beginning of the plateau we determined an average tilt angle of 88° with respect to the layer normal, indicating that molecules are lying flat on the water surface. At the end of the plateau we determined an average tilt angle of the TP cores of 69°. We think that the observed tilt angle of 69° is the average tilt of TP cores being organized in one well-oriented bottom layer in contact with the water surface (90°) and an unoriented upper layer (54°, order parameter of 0; see Figure 11). The upper layer of this arrangement can be understood as one layer of a lamellar-isotropic phase (lam_{iso}),[54−57] which has recently been shown to be a liquid crystalline mesophase in bulk. Such an arrangement cannot be achieved by a "roll-over" mechanism, as it was postulated for several isotherms with similar shape.[5,6,12,13,15,16,25] Rather, the mechanism must be a "lifting" of molecules from the bottom monolayer to the top layer, upon compression. This mechanism has already been discussed in literature.[9−11] Paczesny et al. state that BAM images, taken in the transition regime, are specific for "roll-over" or "lifting" mechanism. Circular domains are an indication for the lifting mechanism, whereas elongated wrinkles are observed when a "roll-over" takes place. According to this theory and the BAM images reported by Reuter et al.,[14] one would predict a "lifting" mechanism for the layering transition of TP 10/3. This assumption can now be confirmed by IRRAS. A new aspect of the results presented herein is that the lifting mechanism does not necessarily lead to a triple-layer arrangement with 3 parallel stacked monolayers, as was previously assumed. By angle dependent IRRAS experiments we showed, that the upper layers of TP 10/3 show a considerable orientational disorder in direction of the surface normal.

Summarizing, we state that neither the existence of a plateau in which the area is reduced to 1/3 of the original value nor a 3-fold increase in layer thickness are sufficient indications for "roll-over" or triple-layer formation.

■ ASSOCIATED CONTENT

Ⓢ Supporting Information

Detailed fitting procedure of the angle dependent IRRA bands as well as simulated and experimental $\nu_s(CH_2)$ bands of TP 16/3 at the 4 positions indicated in Figure 3A (Figure S1−S4). This material is available free of charge via the Internet at http://pubs.acs.org.

■ AUTHOR INFORMATION

Corresponding Author

*E-mail: christian.schwieger@chemie.uni-halle.de.

Notes

The authors declare no competing financial interest.

■ ACKNOWLEDGMENTS

We thank Dr. S. Schwieger for help with the DFT calculations and the Deutsche Forschungsgemeinschaft (DFG) for financial support (FOR 1145).

■ ABBREVIATIONS

TP: terphenyl; A_m: molecular area; AoI: angle of incidence; SmA: smectic A; Col_h: hexagonal columnar; cr: crystalline; ATR: attenuated total reflection; IR: infrared; IRRAS: infrared reflection absorption spectroscopy; BAM: Brewster angle microscopy; AFM: atomic force microscopy; TDM: transition dipole moment; DFT: density functional theory; RT: room temperature

■ REFERENCES

(1) Vontscharner, V.; McConnell, H. M. *Biophys. J.* **1981**, *36*, 409−419.
(2) Phillips, M. C.; Chapman, D. *Biochim. Biophys. Acta* **1968**, *163*, 301−313.
(3) Daniel, M. F.; Lettington, O. C.; Small, S. M. *Thin Solid Films* **1983**, *99*, 61−69.
(4) Demul, M. N. G.; Mann, A. *Langmuir* **1995**, *11*, 3292−3295.
(5) Demul, M. N. G.; Mann, J. A. *Langmuir* **1994**, *10*, 2311−2316.
(6) Diepquang, H.; Ueberreiter, K. *Colloid Polym. Sci.* **1980**, *258*, 1055−1061.
(7) IbnElhaj, M.; Riegler, H.; Mohwald, H. *J. Phys. I* **1996**, *6*, 969−980.
(8) IbnElhaj, M.; Riegler, H.; Mohwald, H.; Schwendler, M.; Helm, C. A. *Phys. Rev. E* **1997**, *56*, 1844−1852.
(9) Modlinska, A.; Inglot, K.; Martynski, T.; Dabrowski, R.; Jadzyn, J.; Bauman, D. *Liq. Cryst.* **2009**, *36*, 197−208.
(10) Niton, P.; Zywocinski, A.; Paczesny, J.; Fialkowski, M.; Holyst, R.; Glettner, B.; Kieffer, R.; Tschierske, C.; Pociecha, D.; Gorecka, E. *Chem. Eur. J.* **2011**, *17*, 5861−5873.
(11) Paczesny, J.; Niton, P.; Zywocinski, A.; Sozanski, K.; Holyst, R.; Fialkowski, M.; Kieffer, R.; Glettner, B.; Tschierske, C.; Pociecha, D.; Gorecka, E. *Soft Matter* **2012**, *8*, 5262−5272.

(12) Plehnert, R.; Schroter, J. A.; Tschierske, C. *Langmuir* **1998**, *14*, 5245−5249.
(13) Plehnert, R.; Schroter, J. A.; Tschierske, C. *Langmuir* **1999**, *15*, 3773−3781.
(14) Reuter, S.; Amado, E.; Busse, K.; Kraska, M.; Stuhn, B.; Tschierske, C.; Kressler, J. *J. Colloid Interface Sci.* **2012**, *372*, 192−201.
(15) Ries, H. E. *Nature* **1979**, *281*, 287−289.
(16) Schroter, J. A.; Plehnert, R.; Tschierske, C.; Katholy, S.; Janietz, D.; Penacorada, F.; Brehmer, L. *Langmuir* **1997**, *13*, 796−800.
(17) Inglot, K.; Martynski, T.; Bauman, D. *Liq. Cryst.* **2006**, *33*, 855−864.
(18) Martynski, T.; Hertmanowski, R.; Bauman, D. *Liq. Cryst.* **2001**, *28*, 437−444.
(19) Jedlovszky, P.; Partay, L. B. *J. Mol. Liq.* **2007**, *136*, 249−256.
(20) O'Neill, M.; Kelly, S. M. *Adv. Mater.* **2011**, *23*, 566−584.
(21) Tschierske, C. *Chem. Soc. Rev.* **2007**, *36*, 1930−1970.
(22) Rapp, B.; Gruler, H. *Phys. Rev. A* **1990**, *42*, 2215−2218.
(23) Bernardini, C.; Cohen Stuart, M. A.; Stoyanov, S. D.; Arnaudov, L. N.; Leermakers, F. A. M. *Langmuir* **2012**, *28*, 5614−5621.
(24) Noll, W.; Steinbac., H; Sucker, C. *J. Polym. Sci., Part C* **1971**, 123−139.
(25) Jeffers, P. M.; Daen, J. *J. Phys. Chem.* **1965**, *69*, 2368−&.
(26) Niton, P.; Zywocinski, A.; Holyst, R.; Kieffer, R.; Tschierske, C.; Paczesny, J.; Pociecha, D.; Gorecka, E. *Chem. Commun.* **2010**, *46*, 1896−1898.
(27) Dutta, A. K. *J. Phys.Chem. B* **1997**, *101*, 569−575.
(28) Plehnert, R.; Schroter, J. A.; Tschierske, C. *J. Mater. Chem.* **1998**, *8*, 2611−2626.
(29) Liu, F.; Chen, B.; Baumeister, U.; Zeng, X.; Ungar, G.; Tschierske, C. *J. Am. Chem. Soc.* **2007**, *129*, 9578−9579.
(30) Hussain, H.; Kerth, A.; Blume, A.; Kressler, J. *J. Phys.Chem. B* **2004**, *108*, 9962−9969.
(31) Tamm, L. K.; Tatulian, S. A. *Q. Rev. Biophys.* **1997**, *30*, 365−429.
(32) Blume, A.; Hübner, W.; Messner, G. *Biochemistry* **1988**, *27*, 8239−8249.
(33) Hunt, R.; Mitchell, M. L.; Dluhy, R. A. *J. Mol. Struct.* **1989**, *214*, 93−109.
(34) Mitchell, M. L.; Dluhy, R. A. *J. Am. Chem. Soc.* **1988**, *110*, 712−718.
(35) Flach, C. R.; Gericke, A.; Mendelsohn, R. *J. Phys. Chem. B* **1997**, *101*, 58−65.
(36) Mendelsohn, R.; Flach, C. R. *Peptide-Lipid Interactions* **2002**, *52*, 57−88.
(37) Chen, B.; Zeng, X. B.; Baumeister, U.; Ungar, G.; Tschierske, C. *Science* **2005**, *307*, 96−99.
(38) Chen, B.; Baumeister, U.; Pelzl, G.; Das, M. K.; Zeng, X. B.; Ungar, G.; Tschierske, C. *J. Am. Chem. Soc.* **2005**, *127*, 16578−16591.
(39) Kuzmin, V. L.; Mikhailov, A. V. *Opt. Spectrosc. (USSR)* **1981**, *51*, 383−385.
(40) Kuzmin, V. L.; Romanov, V. P.; Michailov, A. V. *Opt. Spectrosc.* **1992**, *73*, 1−26.
(41) Flach, C. R.; Gericke, A.; Mendelsohn, R. *J. Phys. Chem. B* **1997**, *101*, 58−65.
(42) Bertie, J. E.; Ahmed, M. K.; Eysel, H. H. *J. Phys. Chem.* **1989**, *93*, 2210−2218.
(43) Bertie, J. E.; Lan, Z. *Appl. Spectrosc.* **1996**, *50*, 1047−1057.
(44) Mendelsohn, R.; Brauner, J. W.; Gericke, A. *Annu. Rev. Phys. Chem.* **1995**, *46*, 305−334.
(45) Mendelsohn, R.; Mao, G. R.; Flach, C. R. *Biochi. Biophys. Acta* **2010**, *1798*, 788−800.
(46) Amado, E.; Kerth, A.; Blume, A.; Kressler, J. r. *Langmuir* **2008**, *24*, 10041−10053.
(47) Xu, Z.; Brauner, J. W.; Flach, C. R.; Mendelsohn, R. *Langmuir* **2004**, *20*, 3730−3733.
(48) Brauner, J. W.; Flach, C. R.; Xu, Z.; Bi, X.; Lewis, R. N. A. H.; McElhaney, R. N.; Gericke, A.; Mendelsohn, R. *J. Phys. Chem. B* **2003**, *107*, 7202−7211.
(49) Dyck, M.; Kerth, A.; Blume, A.; Losche, M. *J. Phys.Chem. B* **2006**, *110*, 22152−22159.
(50) Cameron, D. G.; Casal, H. L.; Mantsch, H. H.; Boulanger, Y.; Smith, I. C. P. *Biophys. J.* **1981**, *35*, 1−16.
(51) Israelachvili, J. N. *Intermolecular and Surface Forces*; Elsevier: Amsterdam, 2011.
(52) Panhuis, M. I. N.; Munn, R. W. *J. Chem. Phys.* **2000**, *113*, 10691−10696.
(53) Bounds, P. J.; Munn, R. W. *Chem. Phys.* **1977**, *24*, 343−353.
(54) Patel, N. M.; Syed, I. M.; Rosenblatt, C.; Prehm, M.; Tschierske, C. *Liq. Cryst.* **2005**, *32*, 55−61.
(55) Cheng, X.; Das, M. K.; Baumeister, U.; Diele, S.; Tschierske, C. *J. Am. Chem. Soc.* **2004**, *126*, 12930−12940.
(56) Cheng, X.; Prehm, M.; Das, M. K.; Kain, J.; Baumeister, U.; Diele, S.; Leine, D.; Blume, A.; Tschierske, C. *J. Am. Chem. Soc.* **2003**, *125*, 10977−10996.
(57) Patel, N. M.; Dodge, M. R.; Zhu, M. H.; Petschek, R. G.; Rosenblatt, C.; Prehm, M.; Tschierske, C. *Phys. Rev. Lett.* **2004**, 92.